Hydrothermal Preparation of Multiwalled Carbon Nanotubes (MWCNTs)/CdS Nanocomposite and Its Efficient Photocatalytic Hydrogen Production under Visible Light Irradiation

ARTICLE *in* ENERGY & FUELS · MAY 2011

Impact Factor: 2.79 · DOI: 10.1021/ef200369z

energy&fuels

ARTICLE

pubs.acs.org/EF

Hydrothermal Preparation of Multiwalled Carbon Nanotubes (MWCNTs)/CdS Nanocomposite and Its Efficient Photocatalytic Hydrogen Production under Visible Light Irradiation

Tianyou Peng,* Peng Zeng, Dingning Ke, Xiaojing Liu, and Xiaohu Zhang

College of Chemistry and Molecular Science, Wuhan University, Wuhan 430072, People's Republic of China

ABSTRACT: Multiwalled carbon nanotubes (MWCNTs)/CdS nanocomposites containing different MWCNT contents were synthesized hydrothermally via direct growth of CdS nanoparticles on the functionalized MWCNT surface. The effects of the hydrothermal temperature and MWCNT content in the nanocomposites on the photoactivity for hydrogen production were investigated comparatively under visible light ($\lambda \geq 420$ nm) irradiation. It was found that 10 wt % MWCNTs/CdS showed much higher photocatalytic hydrogen production efficiency and photostability than the pure CdS nanoparticles. The significantly enhanced photoactivity of the nanocomposite was attributed to the synergetic effect of the intrinsic properties of its components, such as excellent charge transfer and separation on the interfaces between the modified MWCNTs and CdS nanoparticles, resulting from the direct growth of CdS nanoparticles on the MWCNT surface during the hydrothermal process. The present MWCNTs/CdS nanocomposite reveals obvious predominance, such as enhanced visible-light-driven photoactivity and photostability of CdS for hydrogen production.

1. INTRODUCTION

Since the photoelectrochemical splitting of water into H_2 and O_2 on a TiO_2 electrode was first reported in 1972,[1] photocatalytic H_2 production over a semiconductor has been attracting extensive attention because of its potential applications for the production of clean hydrogen energy.[1−6] However, most nanosized oxide semiconductors mainly absorb ultraviolet (UV) because of their wide bandgap (ca. 3.2 eV for anatase TiO_2), which only contains approximately 4% effectiveness of the solar radiant energy.[1,2] Therefore, the development of a novel photocatalyst with high visible light response is indispensable for the photocatalytic H_2 production technique.[3−6]

Cadmium sulfide (CdS), as a visible-light-driven photocatalyst, has been extensively studied because of its excellent water photosplitting property, in that its bandgap (ca. 2.2 eV) corresponds well with the solar spectrum and its conduction band edge is more negative than the H_2O/H_2 redox potential.[7−9] Nevertheless, CdS is prone to photocorrosion during the photochemical reaction because CdS is itself oxidized by the photogenerated holes, which obstruct its large-scale application.[9] Mesoporous silica as a support can improve the photostability of the loaded CdS nanoparticles,[10] but the inorganic matrix may keep the light from reaching CdS. A visible light response material as a matrix of CdS can provide an interface for the charge transfer and then improve the photoactivity for H_2 production.[11]

Recently, carbon nanotubes (CNTs) have attracted considerable attention in the preparation of a nanocomposite with a semiconductor (e.g., TiO_2).[5,12−14] For example, Woan et al.[12] summarized that the CNTs in a CNTs/TiO_2 composite mainly act as a photosensitizer and/or an electron-transfer channel. Kongkanand et al.[13] found that the photogenerated electrons of TiO_2 in the CNTs/TiO_2 composites were transferred to CNTs. Wang et al.[14] prepared a multiwalled carbon nanotubes (MWCNTs)/TiO_2 composite and found that it showed excellent photodegradation efficiency of phenol under visible light illumination. Similarly, efforts have also been devoted to employing CNTs on CdS modification toward binary composites with synergetic effects of their intrinsic properties to increase the photoactivity and photostability of CdS nanoparticles.[15−20] For example, Robel et al.[15] prepared single-walled carbon nanotubes (SWCNTs)/CdS nanocomposites as light-harvesting assemblies and found that the photogenerated electrons of CdS were quickly transferred to CNTs. Cao et al.[16] found that MWCNTs/CdS core−shell nanowires showed much higher photovoltage compared to CdS nanoparticles, ascribed to the CNTs acting as an electron acceptor. Therefore, it has been reported that the CNTs have three main effects. First, CNTs as an electron acceptor could induce an efficient charge transfer and retard the charge recombination.[12,13] Second, as a photosensitizer, CNTs could expand the visible light absorption of the photocatalyst and enhance the visible light use efficiency.[5,14] Moreover, the presence of MWCNTs also hampered the photocorrosion of CdS.[17] However, to the best of our knowledge, there are few investigations focused on MWCNTs/CdS nanocomposites for the photocatalytic H_2 production,[18] although similar material has been used as photocatalysts for the degradation of organic pollution.[17,19]

Herein, we employed a hydrothermal technique to synthesize MWCNTs/CdS nanocomposites by direct growth of CdS on the MWCNT surface. The effects of the hydrothermal condition and the MWCNT content on the crystal phase, morphology, and optical property were investigated in detail. Steady and enhanced visible-light-induced photocatalytic H_2 production efficiency was

Received: March 9, 2011
Revised: April 27, 2011
Published: April 28, 2011

achieved in the present study. Moreover, apparent quantum efficiency (AQE) over the MWCNTs/CdS nanocomposite was determined, and the electron-transfer mechanism for the photocatalytic system containing MWCNTs/CdS was also discussed.

2. EXPERIMENTAL SECTION

2.1. Materials. MWCNTs (diameter, <8 nm; length, 10−30 μm; and purity, >95 wt %) were purchased from Chengdu Organic Chemicals [Chinese Academy of Sciences (CAS), China]. For the purification and surface functionalization, 1.50 g of MWCNTs were dispersed in 65 mL of 3.0 M HNO_3 solution and refluxed for 72 h at 120 °C. After cooling to room temperature, the supernatant was drafted by pipet and then 60 mL of mixed solution of concentrated sulfuric acid and nitric acid (bulk factor = 3:1) was added and refluxed for 4 h under stirring. The resultant MWCNTs were separated, rinsed several times with water until the pH value of the supernatant approached 4.00, and then dried at 60 °C. This pretreatment can generate several functional groups, including hydroxyl, carboxyl, and carbonyl groups, on the MWCNT surface.[17,18] All other chemical reagents used were commercially available with analytical grade and used without further purification.

2.2. Material Preparation. The preparation procedure of MWCNTs/CdS nanocomposite is as follows: an appropriate amount of the functionalized MWCNTs was dispersed by ultrasonication in deionized water to obtain MWCNT suspension (0.6 μg/mL), and then its pH value was adjusted to 10.00 by dropping 0.1 M NaOH solution. A total of 20 mL of 0.03 M $Cd(Ac)_2$ solution was dropped in 30 mL of MWCNT suspension, with stirring for 3 h. Finally, 20 mL of 0.06 M thiourea solution was added to the mixture dropwise under stirring, and then the resultant mixture was transferred to an autoclave for hydrothermal treatment for 5 h at different temperatures. After centrifugation, the product was rinsed with water and ethanol and then dried at 60 °C for 12 h. For comparison, nanocomposites containing different MWCNT contents were also obtained via a similar process.

2.3. Material Characterization. X-ray diffraction (XRD) patterns were obtained with a XRD 6000 diffractometer using Cu Kα radiation (λ = 0.154 18 nm). Scanning electron microscopy (SEM) images were observed on a JSM-6700F electron microscope. Transmission electron microscopy (TEM) images were performed on a Tecnai G2 F20 S-Twin (FEI, Hillsboro, OR). The diffuse reflectance absorption spectra (DRS) were recorded on a Cary 5000 UV−vis−near-infrared (NIR) spectrophotometer equipped an integrating sphere using $BaSO_4$ as a reference. Fourier transform infrared (FTIR) spectra were acquired with a Thermo Nicolet Avatar 360 FTIR spectrometer.

To evaluate the photostability of the photocatalyst, the Cd^{2+} contents in the remnant solutions after the photoreaction and removal of the photocatalyst were detected by a TAS-986 atom absorption spectroscope (Beijing Rayleigh Analytical Instrument Co., Ltd., China). Measurement conditions: GFH-986 graphite furnace; tested wavelength of Cd, 228.8 nm; slit wide, 0.4 nm; lamp current, 1.5 mA; peak height for determination; Ar pressure, 0.4−0.5 MPa; cooling water, >1.5 L/min.

2.4. Photocatalytic Activity Evaluation. Hydrogen production reactions were carried out in an outer irradiation-type photoreactor (Pyrex glass) containing a photocatalyst (e.g., 35 mg of MWCNTs/CdS) and an aqueous solution of 0.35 M Na_2S and 0.25 M Na_2SO_3 (100 mL) as the sacrifice reagent. A 300 W Xe lamp (PLS-SXE300, Beijing Trusttech Co., Ltd., China) was used as the light source, as described in our previous publication.[5,9] A cutoff filter (Kenko L-42, $\lambda \geq 420$ nm) was employed for visible light irradiation. Before the light irradiation, the photoreactor containing the photocatalyst and the sacrificial reagent was sonicated several minutes to let the photocatalyst disperse uniformly and thoroughly degassed to remove air completely. The amount of evolved H_2 was determined by a gas chromatograph [GC, SP-6800A, thermal conductivity detector (TCD), 5 Å molecular sieve columns, and Ar carrier].

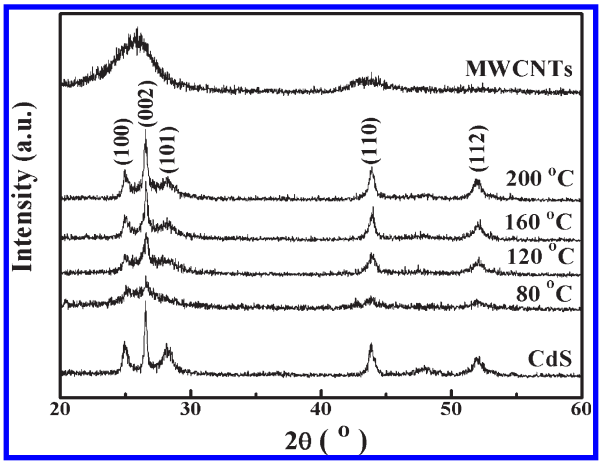

Figure 1. XRD patterns of the 10 wt % MWCNTs/CdS nanocomposites derived from different hydrothermal temperatures.

The AQE was measured under the same photocatalytic reaction condition, except for the incident light wavelength. The hydrogen yields of 1 h photoreaction under different monochromatic light wavelengths (420, 435, 450, 475, 500, 520, and 550 nm) were measured. The band-pass and cutoff filters and a calibrated Si photodiode (SRC-1000-TC-QZ-N, Oriel, Stratford, CT) were used in the above measurement. AQE at different wavelengths is calculated by the following equation:[21]

$$\text{AQE}\ (\%) = \frac{\text{number of reacted electrons}}{\text{number of incident photons}} \times 100$$

$$= \frac{2 \times \text{number of evolved } H_2 \text{ molecules}}{\text{number of incident photons}} \times 100$$

3. RESULTS AND DISCUSSION

3.1. Effects of the Hydrothermal Temperature on the Photocatalytic H_2 Production Efficiency. Figure 1 depicts XRD patterns of 10 wt % MWCNTs/CdS derived from different hydrothermal temperatures. For comparison, pure CdS derived from 160 °C is also depicted in Figure 1. The crystallinity of MWCNTs/CdS is gradually improved upon enhancing the hydrothermal temperature from 80 to 200 °C. The product derived from 80 °C shows relatively weak diffraction peaks attributable to the (100), (002), (110), and (112) crystal planes of the hexagonal CdS [Joint Committee on Powder Diffraction Standards (JCPDS) 751545], but the (101) peak for the hexagonal CdS cannot be observed. After the hydrothermal temperature is enhanced to 120 °C, the product shows an obvious (101) diffraction peak. Upon further enhancement of the hydrothermal temperature to 160 and 200 °C, the products show similar XRD patterns with much higher and sharper diffraction peaks, as compared to the product derived from 120 °C, indicating the crystallinity is improved and the CdS content in the nanocomposite reaches the maximum.[22] The pristine MWCNTs show two broader diffraction peaks at 2θ = 26.2° and 44.6° ascribable to the (110) and (213) planes of MWCNTs, respectively. However, the above diffraction peaks of MWCNTs cannot be obviously observed from the XRD patterns

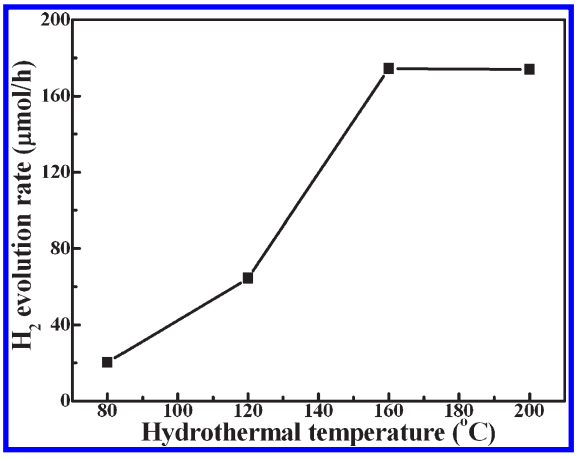

Figure 2. Effects of the hydrothermal temperature on the photocatalytic H_2 evolution efficiency under visible light ($\lambda \geq 420$ nm) irradiation. Conditions: 35 mg of 10 wt % MWCNTs/CdS in 100 mL of suspension containing Na_2S (0.25 M)−Na_2SO_3 (0.35 M).

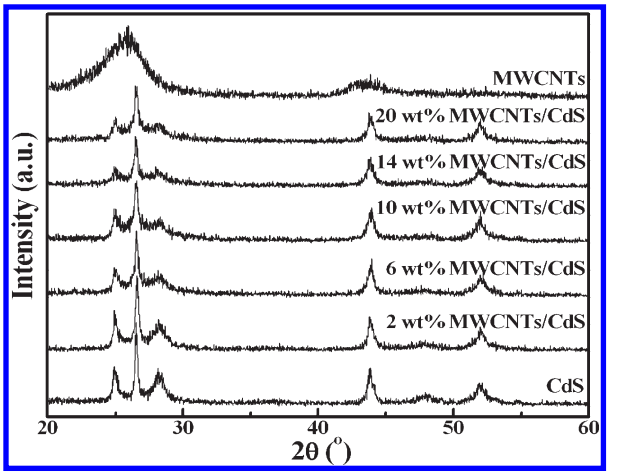

Figure 3. XRD patterns of the MWCNTs, pure CdS nanoparticles, and MWCNTs/CdS nanocomposites with different MWCNT contents.

of the composites because these partly overlap with the (100), (002), and (110) diffraction peaks of CdS, respectively.[15−18]

Figure 2 shows the effects of the hydrothermal temperature on the photocatalytic H_2 production efficiency of 10 wt % MWCNTs/CdS under visible light ($\lambda \geq 420$ nm) irradiation. As can be seen, the product derived from 80 °C shows H_2 production efficiency of 20.2 μmol/h, which markedly increases to 174.2 μmol/h after the hydrothermal temperature is enhanced to 160 °C. Once the hydrothermal temperature is enhanced to 200 °C, the product shows a slightly decreased H_2 production efficiency (173.8 μmol/h). The crystallinity of products derived from 200 °C is slightly higher than that of products derived from 160 °C, as shown in Figure 1. Usually, a higher crystallinity could decrease the crystal defects, retard the charge recombination, and then result in an enhanced photoactivity.[23] Upon enhancement of the hydrothermal temperature, crystallinity of products should be improved, coupled with crystal grain growth, and the increased grain can prolong the charge diffusion distances, which maybe leads to an increased probability of charge recombination and then a decreased photoactivity. Therefore, 160 °C is selected as an optimal hydrothermal temperature for the following investigations.

3.2. Effects of MWCNT Contents on the Nanocomposite Properties. Figure 3 depicts XRD patterns of MWCNTs/CdS nanocomposites derived from 160 °C and different MWCNT contents. As can be seen, all products do not show any obvious peak attributable to the MWCNTs, even for the 20 wt % MWCNTs/CdS. It is consistent with the above XRD observations and can be ascribed to the partial overlapping of the diffraction peaks of the hexagonal CdS.[15−18] The crystal phase of pure CdS is similar to that of the composites under the same hydrothermal temperature, but it shows much higher and sharper diffraction peaks attributable to the hexagonal CdS, indicating pure CdS has better crystallinity.[22] In addition, the peak intensities of the CdS decrease gradually upon enhancing the MWCNT contents. It can be ascribed to the decreased particle size and increased dispersivity of the CdS nanoparticles because of the addition of MWCNTs.

Figure 4 shows the UV−vis DRS of pure CdS, MWCNTs, and MWCNTs/CdS nanocomposites with different MWCNT contents. As can be seen, the onset wavelength for pure CdS is ca.

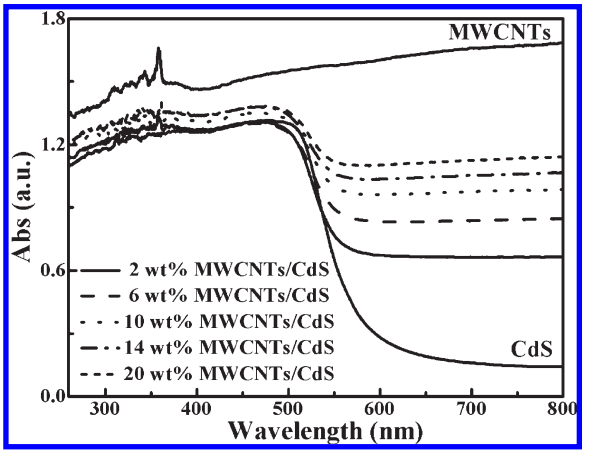

Figure 4. DRS of the MWCNTs, pure CdS nanoparticles, and MWCNTs/CdS nanocomposites with different MWCNT contents.

580 nm, corresponding to a bandgap of 2.11 eV. The pristine MWCNTs show excellent light absorption among the wavelength ranges tested without an obvious absorption peak, which is similar to the previous observation.[5] Although CdS has no absorption above its fundamental absorption edge rising at ca. 580 nm, an apparent enhancement of visible light absorption can be observed for MWCNTs/CdS. Moreover, this enhancement of absorption increases with the enhancement of the MWCNT contents. It could be attributed to the enhancement of the surface electric charge of the CdS in the nanocomposites because of the introduction of MWCNTs, which leads to the possible electronic transition of $\pi \rightarrow \pi^*$ of MWCNTs and $n \rightarrow \pi^*$ between the n orbit of the CdS and MWCNTs.[5,14] This enhancement happens at a wavelength longer than 550 nm and would have influence on the fundamental process of the photogenerated carrier formation and separation in the photocatalytic process.

Figure 5 shows FTIR spectra of pure CdS, MWCNTs, and MWCNTs/CdS. New FTIR peaks centered at 1710 and 1580 cm^{-1} can be observed from the functionalized MWCNTs, as compared to the pristine one (curves g and h of Figure 5), and attributable to the stretching vibrations of C═O and C−C, respectively. It indicates that the present acid pretreatment has

successfully created carboxyl on the MWCNT surface.[5,17,19] The composite with the CdS nanoparticles leads to the carboxylic acid on the MWCNT surface changed into carboxylate, corresponding to the blue shifts for the stretching vibration peaks of COO^-.[19,20] As can be seen from Figure 5b, the peak at 1710 cm^{-1} for −COOH shifts to ∼1740 cm^{-1} coupled with peak weakening, implying that Cd^{2+} has been chemically bonded with $-COO^-$ on the MWCNT surface in the 2 wt % MWCNTs/CdS. In the meantime, the stretching vibration peak ascribable to C−C can also be observed at 1580 cm^{-1}; this peak becomes weakened with a decrease of the MWCNT contents. Therefore, it can be concluded that there are chemical bonding functions among the MWCNTs and CdS nanoparticles in the nanocomposite derived from the present hydrothermal process.[5,17]

3.3. MWCNTs/CdS Morphology Analyses. Figure 6 shows SEM and high-resolution transmission electron microscopy (HRTEM) images of 10 wt % MWCNTs/CdS. As can be seen from Figure 6a, MWCNTs are surrounded by CdS nanoparticles and only less MWCNTs are exposed outside, which is similar to MWCNTs/TiO_2 prepared by a hydrothermal process.[5] CdS nanoparticles show spherical morphology with a particle size ranging 12−28 nm. It also can be observed that not all CdS nanoparticles are bound to the MWCNT surface, which is related to the limited carboxyl groups generated on MWCNTs during the functionalization process.

As can be seen from the HRTEM images in panels b and c of Figure 6, the CdS nanoparticles tightly contacted the MWCNT surface, implying the chemical bonds between the CdS nanoparticles and MWCNTs.[15] Moreover, the CdS nanoparticles on the MWCNT surface have good crystallinity, and the lattice spacing (3.38 Å) corresponds to the interplanar distance of the (002) plane of the hexagonal CdS. The functionlized MWCNTs could first combine with Cd^{2+}, then react with the hydrolysis products of NH_2CSNH_2, and *in situ* form the CdS nanoparticles. Because the solution is relatively static during the hydrothermal process, the local concentration of the rapidly formed S^{2-} is so large and leads to the growth and aggregation of the CdS nanoparticles. Anyway, the chemical bonding between the MWCNTs and CdS nanoparticles would be of benefit to the charge transfer and separation and, thus, enhance its photoactivity for H_2 production,[5,16,17] which will be further discussed in the following sections.

3.4. Effects of MWCNT Contents on the Photocatalytic H_2 Production Efficiency. Control experiments show no appreciable H_2 evolution in the absence of either photocatalyst or light irradiation. Figure 7 shows the time courses of the photocatalytic H_2 evolution over various photocatalysts under visible light

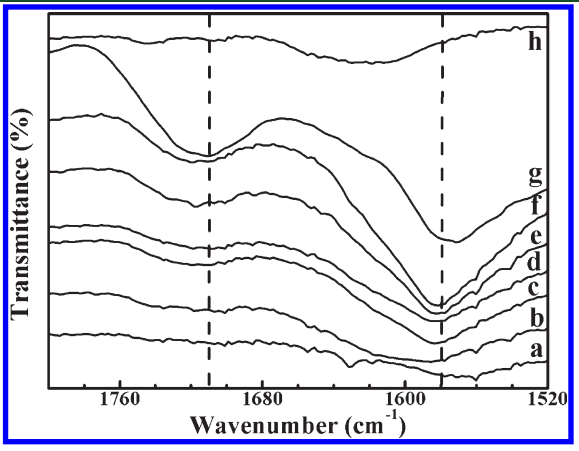

Figure 5. FTIR spectra of the MWCNTs, pure CdS nanoparticles, and MWCNTs/CdS nanocomposites with different MWCNT contents: (a) pure CdS, (b) 2 wt % MWCNTs/CdS, (c) 6 wt % MWCNTs/CdS, (d) 10 wt % MWCNTs/CdS, (e) 14 wt % MWCNTs/CdS, (f) 20 wt % MWCNTs/CdS, (g) functionalized MWCNTs, and (h) pristine MWCNTs.

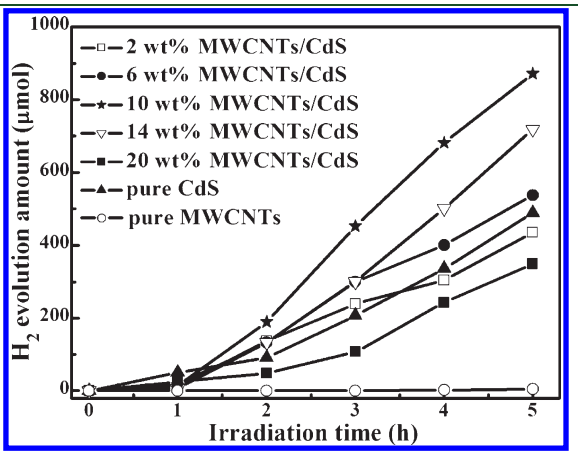

Figure 7. Time courses of the photocatalytic H_2 evolution over the MWCNTs, pure CdS nanoparticles, and MWCNTs/CdS nanocomposites under visible light irradiation ($\lambda \geq 420$ nm).

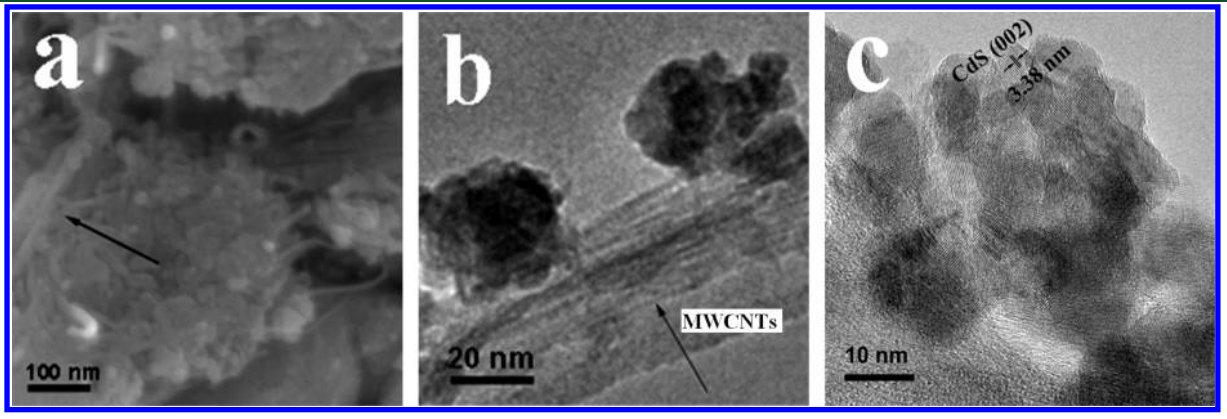

Figure 6. (a) SEM and (b and c) HRTEM images of the 10 wt % MWCNTs/CdS nanocomposite.

irradiation ($\lambda \geq 420$ nm). As can be seen, the functionalized MWCNTs show limited photoactivity for H_2 production. It is similar to the previous reports that almost $^2/_3$ CNTs are semiconductors,[14,18,24] and its bandgap energy may be appropriate to produce H_2 under visible light irradiation. Pure CdS exhibits an average H_2 production rate of 97.9 μmol/h, whereas most nanocomposites exhibit better H_2 production efficiency than pure CdS and MWCNTs under the same conditions, implying that there is an obvious synergetic effect among the components of the nanocomposite because of their excellent chemical bonding between MWCNTs and CdS nanoparticles, which can be readily understood from a chemistry viewpoint. Carboxyl functional groups can be generated on the MWCNT surface after the functionalization and would form MWCNT−COO^- after the NaOH solution treatment. The Cd^{2+} species could react with the anionic species in the mixture (MWNT−COO^-) and, consequently, give birth to the inorganic self-assemblies, and then the CdS nanoparticles could directly grow on the MWCNT surface through tight chemical bonding during the hydrothermal process.

As can be seen from Figure 7, the total amount of H_2 production during the 5 h photoreactions increases upon enhancing the MWCNT contents from 2 to 10 wt % and then decreases with further enhancement to 20 wt %. Namely, 10 wt % MWCNTs/CdS shows an optimal photoactivity with an average H_2 production rate of 174.2 μmol/h, which is about 1.8 times that of pure CdS. When the MWCNT content is small (e.g., 2 wt %), the total amount of H_2 production during the 5 h photoreactions is even lower than that of pure CdS nanoparticles. On one hand, the presence of MWCNTs can lead to the decrease of the relative amount of CdS in the photocatalyst and then to the reduced photogenerated carriers because the same amount (35 mg) of photocatalyst was added in the present photoreaction system. On the other hand, the above-mentioned synergetic effect between MWCNTs and CdS is limited because of the low concentration (2 wt %) of MWCNTs. Therefore, 2 wt % MWCNTs/CdS shows a lower photoactivity than pure CdS.

Upon further enhancement of the MWCNT content ($\leq$10 wt %), the nanocomposite shows increasing photoactivity for H_2 production. The reason is that MWCNTs can act as electron acceptors and transfer channels and enhance the charge separation efficiency.[5,16,17] Once the MWCNT content is larger than 10 wt %, the amount of H_2 production decreases, especially for 20 wt % MWCNTs/CdS. Therefore, it is suitable to conclude that 10 wt % MWCNTs in the composite photocatalyst can act as electron acceptors and transfer channels, efficiently separate the carriers, and then give optimal photocatalytic efficiency, although the absorbance is continuously increased with the enhancement of the CNT contents, as shown in Figure 4. The presence of MWCNTs in the nanocomposite leads to the decrease in the relative amount of CdS as mentioned above and then to the decrease of the photogenerated carriers, because the same amount of photocatalyst was used for the photoreaction, and therefore, the amount of H_2 production decreases especially for the composite containing MWCNTs larger than 10 wt %. Moreover, the absorbance enhancement in the range of 550−800 nm, mainly attributable to the introduction of more MWCNTs, does not necessarily mean an improved photoactivity of CdS according to the undermentioned AQE measurement, which will be further discussed in the following section.

3.5. Preliminary Discussion of the Photocatalytic H_2 Production Mechanism. Three modes of the electron-transfer mechanism have been proposed for the CNT-mediated enhancement of photoactivity in the CNTs/TiO_2 composite:[12] (a) CNTs act as an electron sinks and scavenge away the electrons hindering the charge recombination.[25] (b) The photon can generate electron−hole pairs in the CNTs as proposed by Wang et al.[14] On the basis of the relevant positions of the energy bands, an electron (or the hole) is injected in TiO_2, generating O_2^- or OH• species. (c) CNTs act as an impurity through the Ti−O−C bonds as proposed by Pyrgiotakis et al.,[12] where there are two distinct contributions from the CNTs/TiO_2 composite. One is the C−O−Ti bond that extends the light absorption to longer wavelengths (just like the C-doped TiO_2),[3] thus potentially leading to the improvement of photoactivity. The other is the electron structures of CNTs. They thought that the electronic-band structure of the CNTs is a more important factor than the chemical bond between the CNTs and TiO_2 with regard to the photocatalysis,[12] considering that it is difficult to characterize the electron structures and defects of CNTs and the enhanced photoactivity for the present conditions is under visible light irradiation. Therefore, the explanation on the electron-transfer mechanism for MWCNTs/CdS is based on the former two modes.

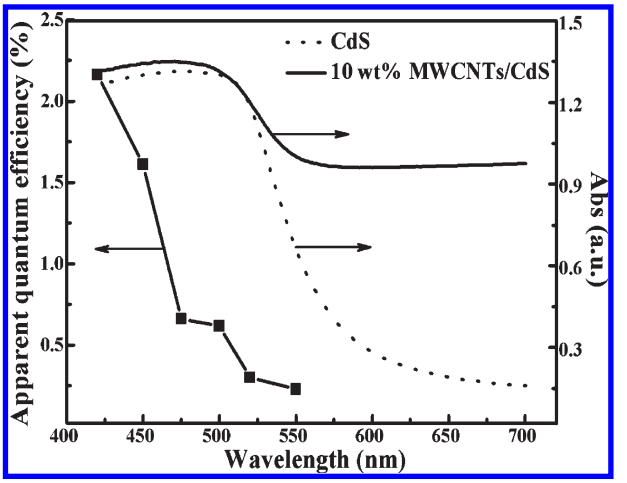

Figure 8. Effects of the wavelength on the AQE for the photocatalytic H_2 production over 10 wt % MWCNTs/CdS from aqueous suspension containing Na_2S (0.25 M)−Na_2SO_3 (0.35 M).

It has been reported that the presence of MWCNTs helps to enlarge the visible light absorption range of CdS.[17] Moreover, MWCNTs have a one-dimensional (1D) carbon-based ideal molecular structures with nanocylinders, in which electrons can be considered to move freely without any scattering from atoms of defects; therefore, it can act as a metal to accept a photogenerated electron and decrease the charge recombination.[17] According to the second mode, CNTs can extend the visible light absorption range of CdS and then improve the photoactivity for H_2 production. As can be seen from the DRS in Figure 4, the absorbance of the nanocomposite in the visible light ranges is enhanced by the addition of MWCNTs. To make clear whether this absorbance enhancement can improve the visible-light-driven photoactivity of CdS or not, AQE for H_2 production over 10 wt % MWCNTs/CdS is determined under different monochromatic light (Figure 8).

The AQE curve for 10 wt % MWCNTs/CdS shows an obviously decreasing trend upon enhancing the wavelength of incident monochromatic light. For example, the AQE for 10 wt % MWCNTs/CdS is 2.16% at 420 nm and then decreases to 0.22%

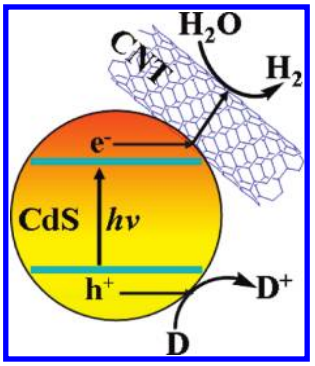

Figure 9. Proposed mechanism for the CNT-mediated enhancement of the photocatalysis process in MWCNTs/CdS. D refer to the electron donor (Na_2S and Na_2SO_3), and CNTs act as an electron sinks to trap electrons and hinder the recombination.

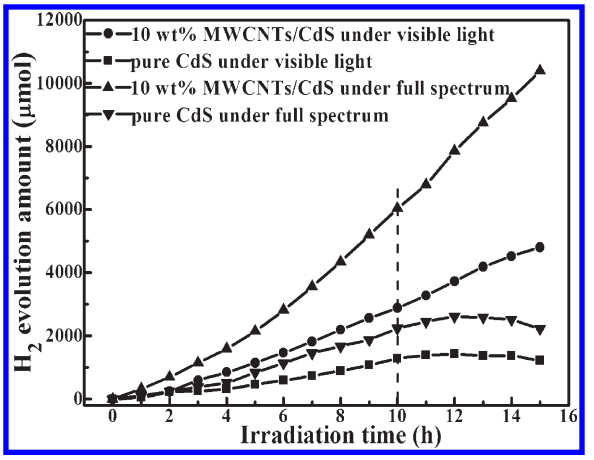

Figure 10. Time courses of the photocatalytic H_2 evolution over MWCNTs/CdS and pure CdS under visible light ($\lambda \geq 420$ nm) and full spectrum of the Xe lamp.

at 550 nm. However, the nanocomposite still shows a relatively strong light absorption at wavelength longer than 550 nm. That is, the AQE curve for 10 wt % MWCNTs/CdS is similar to the DRS of CdS but not the nanocomposite, although it shows a slight blue shift compared to the DRS of CdS. It can be explained by considering that some absorbed light energy is lost because of the carrier recombination during the photocatalytic process.[8] The above results seem to imply that MWCNTs cannot truly extend the light response range of CdS for the photocatalytic H_2 production, although it can enhance the visible light absorption property and even exceed the onset wavelength (ca. 580 nm) of CdS. By considering that MWCNTs can obviously improve the photoactivity for H_2 production, we suggested an electron-transfer mode for MWCNTs/CdS during the photoreactions, as shown in Figure 9, which is similar to the first mode as mentioned above.[18,25]

For the present system, there is a strong interaction between the CdS nanoparticles and MWCNTs. Meanwhile, the long-range π electronic conjugation of MWCNTs is beneficial for accelerating the electron transfer. Thus, the photogenerated electrons of CdS can be transferred quickly to MWCNTs under light irradiation[16] and then to generate H_2. The remnant holes in the valence bands of CdS can react with sacrificial reagent. Therefore, MWCNTs can help with the separation of the carriers produced by CdS and improve the photoactivity. Many researches also found that CNTs can act as an electron acceptor. For example, Robel et al.[15] reported that the excited states of CdS can be rapidly quenched when CdS nanoparticles are chemically bonded with SWCNTs and thought that the electrons could be transferred to SWCNTs.[15] Recently, Kongkanand et al.[13] found that SWCNTs can accept and deposit the electrons of TiO_2 in a photoelectrochemical solar cell (1 electron for every 32 carbon atoms). Moreover, Cao et al.[16] confirmed that the disassociation of photogenerated species is more efficient in the MWCNTs/CdS core−shell nanowires because of the photoinduced charge transfer from CdS to the CNTs. Therefore, it can be concluded that the improved photocatalytic H_2 evolution efficiency of 10 wt % MWCNTs/CdS can be attributed to the synergetic effect of the two components, such as excellent charge transfer and separation. On the other hand, MWCNTs can also produce limited H_2, as shown in Figure 7, indicating that it can also absorb the visible light, and the electrons of excited MWCNTs can be used for the H_2 production.[5] Namely, the enhanced photoactivity for H_2 production of MWCNTs/CdS is probably attributed to the photosensitization mechanism to some extent. However, very low AQE at 550 nm seems not to support the above supposition; at least the contribution for H_2 production through the photosensitization of MWCNTs is very limited in the present system, which needs to be further investigated.

3.6. Photocatalytic H_2 Evolution Stability. Figure 10 shows the time course of photocatalytic H_2 evolution over 10 wt % MWCNTs/CdS and CdS under the visible light or full spectrum of the Xe lamp. As can be seen, 10 wt % MWCNTs/CdS shows much higher photoactivity than pure CdS. Under visible light irradiation, the total amount of H_2 production for 10 wt % MWCNTs/CdS is up to 2882.8 μmol after 10 h of photoreaction, which is 2.25 times that of pure CdS. Under full spectrum, the obviously increased amount of H_2 production for both MWCNTs/CdS and CdS nanoparticles can be observed. The total amount of H_2 production up to 6031.6 μmol for 10 wt % MWCNTs/CdS is achieved after 10 h of photoreaction, which is 2.70 times that of pure CdS. However, the total amounts of H_2 production for pure CdS show decreasing trends after more than 11 h of irradiation under both visible light and full spectrum, and the amount of H_2 production for pure CdS under full spectrum shows a more obvious decreasing trend than that under visible light. The possible reason may be that the CdS nanoparticles are more easily corrosive under full spectrum of the Xe lamp, whereas 10 wt % MWCNTs/CdS can remain steady, increasing the H_2 production amount, implying its good photostability.

It is noticeable that the initial amount of H_2 production for 10 wt % MWCNTs/CdS is slightly low. After the photoreaction time is larger than 2 h, the amount of H_2 production increased obviously. According to the above analyses, MWCNTs cannot only act as an electron-transfer channel but also deposit the electrons. Under the initial stage, some photogenerated electrons can be deposited by the MWCNTs,[13] and therefore, the initial photoactivity is low. Upon a prolonged irradiation time, more electrons can be used to produce H_2 because of the limited electron deposition amount of the MWCNTs, when leads to the gradual enhancement of the photoactivity. The suspension after 10 h of photoreaction is centrifugally separated from 10 wt % MWCNTs/CdS under both visible light and full spectrum irradiation, and the Cd^{2+} amount in the solution is determined via atom absorption spectroscopy to verify the photocorrosion of CdS. There is no obvious Cd^{2+} detected in the photoreaction

solution after removal of 10 wt % MWCNTs/CdS. Moreover, the Cd^{2+} amount in the photoreaction solution after 15 h of visible light irradiation was also detected for all nanocomposites. The Cd^{2+} concentrations in the photoreaction solutions after removal of 0, 2, 6, 10, 14, and 20 wt % MWCNTs/CdS nanocomposites are 10.6, 2.02, 0.22, 0, 0, and 0 μg/mL, respectively. The above results also validated that MWCNTs/CdS has good photostability during the photoreaction. Namely, MWCNTs can effectively hamper the photocorrosion of CdS as described above.

It has been reported that a reducing agents (such as S^{2-}, SO_3^{2-}, or $S_2O_3^{2-}$) used as a hole scavenger in aqueous solution suspension had the ability to stabilize CdS nanoparticles.[8] The reason for the present inhibition effect of MWCNTs on the photocorrosion of CdS may be that MWCNTs could function as a support or dispersing agent to enlarge the surface area of the composites, resulting in a higher adsorption capacity for the hole scavenger (Na_2S and Na_2SO_3) in the present photoreaction solution.[17] Therefore, the higher the adsorption capacity of the photocatalyst, the more stable the CdS nanoparticles, because there would be more hole scavengers on the surface of photocatalysts to capture holes for the prevention of the photocorrosion, which is similar to the situation that incorporating CdS nanoparticles into some organic or inorganic matrixes with porous structures had the ability to stabilize and immobilize the CdS nanoparticles.[9,10] Apparently, the above results suggest interesting possibilities for the preparation of efficient visible-light-driven photocatalysts with better durability in comparison to organic dye-sensitized semiconductors.[26] The good interfacial combination between the two components is helpful to hinder the backward electron transfer and improve the quantum efficiency. From the present facile process, the unique properties of MWCNTs can be used by coupling with not only CdS but also many other semiconductors, which is potential for obtaining enhanced photoactivity for H_2 production and pollutant degradation.

4. CONCLUSION

A series of MWCNTs/CdS nanocomposites with different MWCNT contents were successfully synthesized via direct growth of CdS nanoparticles on the functionalized MWCNT surface by a hydrothermal method. The experimental results demonstrate that most of MWCNTs/CdS composites show higher photoactivity than pure CdS and 10 wt % MWCNTs/CdS derived from 160 °C shows the maximum photocatalytic H_2 production efficiency because of its fast carrier separation. Carboxyl on the MWCNT surface would help the achievement of direct chemical bonding between MWCNTs and the CdS nanoparticles, resulting in the synergistic effect of CNTs and CdS. After the comparison to the AQE and absorption spectra of MWCNTs/CdS, it can be concluded that MWCNTs can enhance the photoactivity and photostability of CdS because MWCNTs not only suppress the photogenerated carrier recombination as an electron-transfer channel and acceptor but also stabilize CdS in the aqueous solutions as a support. The present investigation indicates that the MWCNTs/CdS nanocomposites are efficient visible-light-driven photocatalysts with better durability because of their efficient chemical bonding between MWCNTs and CdS, which leads to enhanced charge transfer and separation efficiency and is potential for developing efficient photocatalysts for H_2 production and pollutant degradation.

AUTHOR INFORMATION

Corresponding Author

*Telephone/Fax: 86-27-6875-2237. E-mail: typeng@whu.edu.cn.

ACKNOWLEDGMENT

This work is supported by the Natural Science Foundation of China (20973128), the Program for New Century Excellent Talents in University (NCET-07-0637), and the Fundamental Research Funds for the Central Universities (2081003) of China.

REFERENCES

(1) Fujishima, A.; Honda, K. Electrochemical photolysis of water at a semiconductor electrode. *Nature* **1972**, *238*, 37–38.

(2) Yi, H. B.; Peng, T. Y.; Ke, D. N.; Dai, K.; Zan, L.; Yan, C. H. Photocatalytic H_2 production from methanol aqueous solution over titania nanoparticles with mesostructures. *Int. J. Hydrogen Energy* **2008**, *33*, 672–678.

(3) Khan, S. U. M.; Al-Shahry, M.; Ingler, W. B. Efficient photochemical water splitting by a chemically modified *n*-TiO_2. *Science* **2002**, *297*, 2243–2244.

(4) Zou, Z. G.; Ye, J. H.; Sayama, K.; Arakawa, K. Direct splitting of water under visible light irradiation with an oxide semiconductor photocatalyst. *Nature* **2001**, *414*, 625–627.

(5) Dai, K.; Peng, T. Y.; Ke, D. N.; Wei, B. Q. Photocatalytic hydrogen generation using a nanocomposite of multi-walled carbon nanotubes and TiO_2 nanoparticles under visible light irradiation. *Nanotechnology* **2009**, *20*, No. 125603.

(6) Lv, H. J.; Ma, L.; Zeng, P.; Ke, D. N.; Peng, T. Y. Synthesis of floriated $ZnFe_2O_4$ with porous nanorod structures and its photocatalytic hydrogen production under visible light. *J. Mater. Chem.* **2010**, *20*, 3665–3672.

(7) Jing, D. W.; Guo, L. J. A novel method for the preparation of a highly stable and active CdS photocatalyst with a special surface nanostructure. *J. Phys. Chem. B* **2006**, *110*, 11139–11145.

(8) Bao, N. Z.; Shen, L. M.; Takata, T.; Domen, K. Self-templated synthesis of nanoporous CdS nanostructures for highly efficient photocatalytic hydrogen production under visible light. *Chem. Mater.* **2008**, *20*, 110–117.

(9) Ke, D. N.; Liu, S. L.; Dai, K.; Zhou, J. P.; Zhang, L. N.; Peng, T. Y. CdS/regenerated cellulose nanocomposite films for highly efficient photocatalytic H_2 production under visible light irradiation. *J. Phys. Chem. C* **2009**, *113*, 16021–16026.

(10) Ryu, S. Y.; Balcerski, W.; Lee, T. K.; Hoffmann, M. R. Photocatalytic production of hydrogen from water with visible light using hybrid catalysts of CdS attached to microporous and mesoporous silicas. *J. Phys. Chem. C* **2007**, *111*, 18195–18203.

(11) Koca, A.; Sahin, M. Photocatalytic hydrogen production by direct sun light from sulfide/sulfite solution. *Int. J. Hydrogen Energy* **2002**, *27*, 363–367.

(12) Woan, K.; Pyrgiotakis, G.; Sigmund, W. Photocatalytic carbon nanotube−TiO_2 composites. *Adv. Mater.* **2009**, *21*, 2233–2239.

(13) Kongkanand, A.; Kamat, P. V. Electron storage in single wall carbon nanotubes. Fermi level equilibration in semiconductor−SWCNT suspensions. *ACS Nano* **2007**, *1*, 13–21.

(14) Wang, W. D.; Serp, P.; Kalck, P.; Faria, J. L. Visible light photodegradation of phenol on MWNT−TiO_2 composite catalysts prepared by a modified sol−gel method. *J. Mol. Catal. A: Chem.* **2005**, *235*, 194–199.

(15) Robel, I.; Bunker, B. A.; Kamat, P. V. Single-walled carbon nanotube−CdS nanocomposites as light-harvesting assemblies: Photoinduced charge-transfer interactions. *Adv. Mater.* **2005**, *17*, 2458–2463.

(16) Cao, J.; Sun, J. Z.; Hong, J.; Li, H. Y.; Chen, H. Z.; Wang, M. Carbon nanotube/CdS core−shell nanowires prepared by a simple room-temperature chemical reduction method. *Adv. Mater.* **2004**, *16*, 84–87.

(17) Ma, L. L.; Sun, H. Z.; Zhang, Y. G.; Lin, Y. L.; Li, J. T.; Wang, E.; Yu, Y.; Tan, M.; Wang, J. B. Preparation, characterization and photocatalytic properties of CdS nanoparticles dotted on the surface of carbon nanotubes. *Nanotechnology* **2008**, *19*, No. 115709.

(18) Kim, Y. K.; Park, H. Light-harvesting multi-walled carbon nanotubes and CdS hybirds: Application to photocatalytic hydrogen production from water. *Energy Environ. Sci.* **2011**, *4*, 685–694.

(19) Cai, Z. X.; Yan, X. P. In situ electrostatic assembly of CdS nanoparticles onto aligned multiwalled carbon nanotubes in aqueous solution. *Nanotechnology* **2006**, *17*, 4212–4216.

(20) Huang, Q.; Gao, L. Synthesis and characterization of CdS/multiwalled carbon nanotube heterojunctions. *Nanotechnology* **2004**, *15*, 1855–1860.

(21) Kudo, A.; Miseki, Y. Heterogeneous photocatalyst materials for water splitting. *Chem. Soc. Rev.* **2009**, *38*, 253–278.

(22) Wang, C.; Ao, Y. H.; Wang, P. F.; Hou, J.; Qian, J.; Zhang, S. H. Controlled synthesis in large-scale of CdS mesospheres and photocatalytic activity. *Mater. Lett.* **2009**, *64*, 439–441.

(23) Jang, J. S.; Joshi, U. A.; Lee, L. S. Solvothermal synthesis of CdS nanowires for photocatalytic hydrogen and electricity production. *J. Phys. Chem. C* **2007**, *111*, 13280–13287.

(24) Saito, R.; Fujita, M. Electronic structure and growth mechanism of carbon tubules. *Mater. Sci. Eng., B* **1993**, *19*, 185–191.

(25) Hoffmann, M. R.; Martin, S. T.; Choi, W.; Bahnemann, D. W. Environmental applications of semiconductor photocatalysis. *Chem. Rev.* **1995**, *95*, 69–96.

(26) Peng, T. Y.; Ke, D. N.; Cai, P.; Dai, K.; Ma, L.; Zan, L. Influence of different ruthenium(II) bipyridyl complex on the photocatalytic H_2 evolution over TiO_2 nanoparticles with mesostructures. *J. Power Source* **2008**, *180*, 498–505.